USC–SIPI REPORT #212

Fractal Estimation from Noisy Measurements via Discrete Fractional Gaussian Noise (DFGN) and the Haar Basis

by

Lance M. Kaplan and C.-C. Jay Kuo

July 1992

Signal and Image Processing Institute
UNIVERSITY OF SOUTHERN CALIFORNIA
Department of Electrical Engineering-Systems
3740 McClintock Avenue, Room 400
Los Angeles, CA 90089-2564 U.S.A.

Fractal Estimation from Noisy Measurements via Discrete Fractional Gaussian Noise (DFGN) and the Haar Basis *

Lance M. Kaplan † and C.-C. Jay Kuo †

July 28, 1992

EDICS 5.2.1 or 4.8

Abstract

In this research we first show that when the increments of sampled fractional Brownian motion (fBm), also known as discrete fractional Gaussian noise (DFGN), is set equal to the finest scale wavelet approximation coefficients and when the Haar basis is selected, the discrete wavelet transform (DWT) coefficients are weakly correlated and have a variance that is exponentially related to scale. Similar results were derived by Flandrin, Tewfik and Kim for a continuous-time fBm going through a continuous wavelet transform (CWT), and the theoretical results justify a fractal estimation algorithm recently proposed by Wornell and Oppenheim. However, since discrete samples of fBm data are passed through the DWT in practice, Wornell and Oppenheim's algorithm may not yield an accurate estimate. Thus, motivated by our theoretical result, a new fractal estimation algorithm is proposed by handling the increments of the sampled fBm rather than the sampled fBm itself. The performance of the new algorithm is compared with that of Wornell and Oppenheim's algorithm in numerical simulation.

1 Introduction

To model stochastic processes that exhibit significant correlation for large lags, Mandelbrot and Van Ness [10] introduced fractional Brownian motion (fBm) which is a generalization of normal Brownian motion. The fBm $B_H(t)$ is a zero mean nonstationary Gaussian random process with the covariance function

$$r_{B_H}(t,s) = \frac{\sigma^2}{2}[|t|^{2H} + |s|^{2H} - |t-s|^{2H}], \tag{1.1}$$

*This work was supported by a National Science Foundation Fellowship and a National Science Foundation Young Investigator Award.

†The authors are with the Signal and Image Processing Institute and the Department of Electrical Engineering-Systems, University of Southern California, Los Angeles, California 90089-2564. E-mail: lancekap@sipi.usc.edu and cckuo@sipi.usc.edu.

where the parameters σ^2 and $0 < H < 1$ characterize the process. The parameter H controls the "roughness" of the fBm such that an individual realization of the process has a fractal dimension [9]

$$D = 2 - H.$$

The H parameter also controls the shape of the average spectral density defined as [2]

$$S(f) = \frac{c}{|f|^{\gamma_b}},$$

where

$$\gamma_b = 2H + 1. \tag{1.2}$$

As a result, the fBm serves as a good model for $1/f$ processes where $1 < \gamma_b < 3$, which represents the infrared (IR) catastrophe case [18]. The IR case is the most common case of $1/f$ processes, and many examples of these $1/f$ processes can be found in nature and even economics [6].

The continuous-time fBm is of only theoretical interest. For practical computation, we have to sample the continuous-time fBm via

$$B[k] = B_H(k\Delta x), \quad k \in \mathbf{Z}, \tag{1.3}$$

where Δx is the sampling period. The increment

$$X[k] = B[k+1] - B[k] \tag{1.4}$$

defines a sequence known as the discrete fractional Gaussian noise (DFGN). The variance of the fBm has a self-similar property which provides a variance relation of [7]:

$$\mathrm{var}(B[k+p] - B[k]) = p^{2H}|\Delta x|^{2H}\mathrm{var}(B[k+1] - B[k]). \tag{1.5}$$

It can also be shown [7] that the DFGN is a zero mean stationary Gaussian process that is characterized by its autocorrelation

$$r[k] = \frac{\sigma^2}{2}|\Delta x|^{2H}[|k+1|^{2H} + |k-1|^{2H} - 2|k|^{2H}]. \tag{1.6}$$

Without loss of generality, we set $\Delta x = 1$ for the following discussion.

The estimation of the fractal dimension of the continuous-time fBm from its real discrete data is a very important problem, which can be applied to linear prediction problems and texture classification [7]. Many fractal estimation techniques exist [4], [7], [12], but

they cannot handle noisy measurements. Tewfik and Deriche [14] examined a maximum likelihood estimator that handles noise and some discrete-time fBm of a form different from (1.4). Most of the fractal estimators use regression analysis to take advantage of the exponential progressions, which are characteristics of fractals, in the frequency or space domain. In fact, it has been shown by Flandrin [3] and Tewfik and Kim [16] that the continuous wavelet transform (CWT) coefficients of the continuous-time fBm are weakly correlated and have an exponential variance progression per scale. As a result, estimators can be designed using wavelets. Wornell and Oppenheim [18] took full advantage of the whitening effect of the wavelet transform to derive a maximum likelihood estimator when a $1/f$ process is embedded in white Gaussian noise. Some discussion on the Wornell and Oppenheim's algorithm will be given in Section 2.

The variance progression is however based on the continuous wavelet transform (CWT), and since for most cases only discrete samples of the fBm are available, the discrete wavelet transform (DWT) must be utilized. The sampled data are usually used as the initial approximation wavelet coefficients. For such a case, it has been shown that the variance progression of the coefficients is biased [3], and the bias leads to an underestimate of H. To fix the problem, we first show in Section 3 that when the increments of the sampled fBm (or the DFGN), is set equal to the finest scale wavelet approximation coefficients and when the Haar basis is selected, the DWT coefficients are weakly correlated and have a variance that is exponentially related to scale. Then, we discuss in Section 4 a modified fractal estimation algorithm by using the DFGN and the Haar wavelet transform. The new algorithm will be compared with the algorithm of Wornell and Oppenheim in Section 5, and Section 6 concludes the paper.

2 Discussion on Wornell and Oppenheim's Algorithm

Wornell and Oppenheim's algorithm first passes sampled $1/f$ noise measurements through the DWT based on an algorithm of Mallat [8]. That is, given a sampled signal $a_0[k]$ of the finest scale $m = 0$, we calculate the approximation coefficients $a_m[k]$, and the detail coefficients $d_m[k]$ of coarser scale $m > 0$ recursively via

$$a_{m+1}[k] = \sum_{k'=-\infty}^{\infty} h[2k - k']a_m[k'], \tag{2.1}$$

$$d_{m+1}[k] = \sum_{k'=-\infty}^{\infty} g[2k - k']a_m[k'], \tag{2.2}$$

where $h[k]$ and $g[k]$ must satisfy the quadrature mirror filter (QMF) constraint, i.e. $g[k] = (-1)^k h[1-k]$. Then, the average power, or variance, of the wavelet coefficients, $d_m[k]$, for each scale is calculated. Finally, the variance estimates are put through an estimate-maximize (EM) algorithm to find the maximum likelihood estimate of H. The EM algorithm is based on the fact that the wavelet coefficients are uncorrelated and that for a given scale, the variance of the coefficients is

$$\text{var}[d_m[k]] = \sigma^2 2^{\gamma_b m} + \sigma_w^2, \tag{2.3}$$

where γ_b is related to H via (1.2) and σ_w^2 is the variance of the initial white noise process. The algorithm also estimates σ^2 and σ_w^2. The results of these estimates, however, are of no concern in this paper. The EM algorithm can be tuned for three modes: σ_w^2 is unknown, $\sigma_w^2 > 0$ is known, and $\sigma_w^2 = 0$ is known.

To be of practical value, the filter responses $h[k]$ and $g[k]$ in (2.1) and (2.2) should have compact support. Daubechies [1] studied a family of bases of length $2R$ that satisfy the QMF constraint and have R vanishing moments. For the case $R = 1$, the basis is simply the Haar basis with a filter length of 2, i.e. $h[n] = (\sqrt{2})^{-1}$ for $n = 0, 1$ and 0 otherwise. When the basis function has support of length greater than 2, not all wavelet coefficients can be computed exactly, because there is only a finite number of sampled signals of the finest scale available. For this case, it is often that the DWT computation assumes periodic extension of available data. However, the extrapolation method may cause some harmful effects.

Wornell justified the variance progression in (2.3) by arguing that the wavelet transform acts as a Karhunen-Loève-like expansion for $1/f$ noise [17]. That is, if $d_m[k]$ is indeed uncorrelated over scale and time and if the variance progression of the coefficients does follow (2.3) where $\sigma_w^2 = 0$, then the actual process is nearly $1/f$ in the sense that the power spectrum is bounded:

$$\frac{c_1}{|f|^{\gamma_b}} \leq S(f) \leq \frac{c_2}{|f|^{\gamma_b}}.$$

The variance progression was also validated in [16], where it is proved that if fBm is passed through a continuous wavelet transform then (2.3) is correct and that the $d_m[k]$ terms are weakly correlated in scale and time. To be precise, the cross correlation of $d_m[k]$ and $d_n[l]$ decays asymptotically as

$$E[d_m[k]d_n[l]] \sim O(|2^m k - 2^n l|^{2(H-R)}), \tag{2.4}$$

where R is the number of vanishing moments of the selected wavelet basis.

Consequently, the wavelet basis must be selected such that $R \geq 2$ to whiten the fBm, which means the support of the basis must be at least of length 4 [1]. Errors in the computation of Wornell's algorithm appear because not all wavelet coefficients can be computed exactly for finite supported fBm by using a wavelet basis of length at least 4. Besides, Wornell and Oppenheim's algorithm must perform the DWT on the discretely sampled fBm. Then, the variance progression of (2.3) for the wavelet coefficients is biased and this error leads to an under estimate of the parameter H when only a small amount of measurements are available [3].

3 Properties of DWT Coefficients of DFGN Using Haar Basis

Wornell and Oppenheim's algorithm uses the sampled fBm which is a nonstationary process and can be generated by the DFGN. Since the sampled fBm and the DFGN are causally invertible, they share the same amount of information. By applying the CWT to the fBm, the nonstationarity falls into the CWT coefficients. For the DWT case, however, even though the wavelet coefficients are stationary for the Haar basis, the recursive computation of the coefficients causes the nonstationarity to propagate through scale and bias the variance progression. As a fix to the problem, we consider the application of the DWT to the DFGN.

3.1 Theory

In this section, we will show that when the finest approximation coefficients are set to be equal to the DFGN, the DWT coefficients have many desirable properties. Roughly speaking, they follow a nice variance progression per scale, and as lag increases, the correlation of the coefficients decay much faster than that of the correlation of the DFGN. To make the correlation comparison, it is instructive to perform a Taylor series expansion on (1.6) to understand the asymptotic decay of $r[k]$. The following Taylor series expression is very useful:

$$|1 + \frac{\alpha}{t}|^{2H} = \sum_{r=0}^{\infty} \frac{\alpha^r}{r!} V(r) |t|^{-r} \tag{3.1}$$

where

$$V(r) = \prod_{s=0}^{r-1} (2H - s).$$

Then, by substituting (3.1) into (1.6), we can express $r[k]$ as

$$r[k] = \frac{\sigma^2}{2}|k|^{2H} \sum_{r=1}^{\infty} \frac{2}{(2r)!} V(2r)|k|^{-2r}. \tag{3.2}$$

The rate of decay of $r[k]$ is controlled by the first coefficient of the summation. The Taylor series expansion in (3.2) helps to demonstrate the whitening effect of the DWT. The properties of the wavelet coefficients are stated and proved below.

Theorem 1 *Let $B[k]$ be sampled fBm with a parameter $0 < H < 1$, and $h[n]$ and $g[n]$ be the scaling and wavelet filter realizations of the Haar basis as given in (2.1) and (2.2). Define the stochastic process $d_m[k]$ as the detail wavelet coefficients of the DWT where the finest scale approximation $a_0[k]$ is the increment $X[k] = B[k+1] - B[k]$ of the sampled fBm. Then,*

(a) for fixed scale m the variance of $d_m[k]$ is

$$\text{var}[d_m[k]] = 2^{\gamma(m-1)}\sigma^2(2 - 2^{\gamma}), \tag{3.3}$$

where

$$\gamma = 2H - 1; \tag{3.4}$$

(b) for fixed scale m the autocorrelation $r_{d_m}[k-l]$ of $d_m[k]$ decays as $O(|k-l|^{2(H-2)})$ for all k, l such that $|k-l| > 0$.

Proof: Since $a_0[k] = X[k]$, the autocorrelation of $a_0[k]$ is given by (1.6). First, we want to show that the autocorrelation $r_{a_m}[k]$ of the approximation coefficients $a_m[k]$ for scale $m \geq 0$ as calculated via (2.1) is related to the autocorrelation $r[k]$ of the increments $X[k]$ by

$$r_{a_m}[k] = 2^{(2H-1)m} r[k]. \tag{3.5}$$

It is obvious that (3.5) holds for $m = 0$. Let us assume

$$r_{a_{m-1}}[k] = 2^{(2H-1)(m-1)} r[k]. \tag{3.6}$$

Due to (2.1) and the Haar basis, we have

$$a_m[k] = \frac{1}{\sqrt{2}}(a_{m-1}[2k] + a_{m-1}[2k+1]). \tag{3.7}$$

By combining (3.6) and (3.7) , it is easy to show that the autocorrelation of $a_m[k]$ is

$$r_{a_m}[k] = \frac{2^{(2H-1)(m-1)}}{2}(2r[2k] + r[2k+1] + r[2k-1]). \tag{3.8}$$

By substituting (1.6) into (3.8), one obtains

$$r_{a_m}[k] = 2^{(2H-1)m}\frac{\sigma^2}{2}(|k+1|^{2H} + |k-1|^{2H} - 2|k|^{2H}) = 2^{(2H-1)m}r[k].$$

Thus, by induction, (3.5) holds for all $m \geq 0$. Next, we examine the autocorrelation $r_{d_m}[k]$ of the detail coefficients $d_m[k]$. From (2.2) and the Haar basis,

$$d_m[k] = \frac{1}{\sqrt{2}}(a_{m-1}[2k] - a_{m-1}[2k+1]). \tag{3.9}$$

By combining (3.5) and (3.9), one gets

$$r_{d_m}[k] = \frac{2^{(2H-1)(m-1)}}{2}(2r[2k] - r[2k+1] - r[2k-1]). \tag{3.10}$$

Thus, (3.3) is obtained by setting $k = 0$ in (3.10) and using (1.6), and Part (a) is proved.

Substitution of (1.6) in (3.10) yields

$$r_{d_m}[k] = \frac{2^{(2H-1)(m-1)}}{2}\frac{\sigma^2}{2}(4|2k+1|^{2H} + 4|2k-1|^{2H} - |2k+2|^{2H} - |2k-2|^{2H} - 6|2k|^{2H}). \tag{3.11}$$

By factoring out the $2k$ term in (3.11) and using the Taylor series expansion (3.1), we have

$$r_{d_m}[k] = 2^{(2H-1)m}\frac{\sigma^2}{2}|k|^{2H}\sum_{r=0}^{\infty}\frac{P(r)}{r!}V(r)|k|^{-r}, \tag{3.12}$$

where

$$P(r) = 4(\frac{1}{2})^r + 4(-\frac{1}{2})^r - 1 - (-1)^r - 6\delta(r).$$

Since

$$P(r) = 0 \text{ for } r = 0, 1, 2, 3,$$

the autocorrelation of $d_m[k]$ decays as expressed in Part (b). □.

It is worthwhile to point out several features for the above result. First, the scaling filter (2.1) of the Haar basis takes full advantage of the self-similarity of the fBm as characterized by (1.5). In particular, for approximation coefficients $a_m[k]$, each increase in scale m is like subsampling the fBm by a factor of two and, due to (1.6), a 2^{2H} term pops up in the expression for the correlation of $a_m[k]$ by doubling the value of k. Note also that the fBm increment $X[k]$ approximates the first-order differentiation so that the asymptotic behavior

of the DFGN correlation from (3.2) is $O(|k|^{2H-2})$ and the variance progression is governed by (3.4) rather than (1.2). Finally, the regularity of the Haar wavelet filter causes the first term in the Taylor series expansion in (3.2) to disappear. Theorem 1 can be generalized below for the correlation $r_d[m,n;k,l]$ of $d_m[k]$ and $d_n[l]$ between scales m and n.

Theorem 2 *Let $B[k]$ be sampled fBm with a parameter $0 < H < 1$, and $h[n]$ and $g[n]$ be the scaling and wavelet filter realizations of the Haar basis as given in (2.1) and (2.2). Define the stochastic process $d_m[k]$ as the detail wavelet coefficients of the DWT where the finest scale approximation $a_0[k]$ is the increment $X[k] = B[k+1] - B[k]$ of the sampled fBm. Then,*

(a) The correlation $r_d[m,n;k,l]$ of $d_m[k]$ and $d_n[l]$ is

$$\begin{aligned} r_d[m,n;k,l] &= E[d_m[k]d_n[l]] = \frac{\sigma^2}{2}2^{-\frac{m+n}{2}}(2|2^m k - 2^n l + 2^m - 2^{n-1}|^{2H} \\ &\quad +2|2^m k - 2^n l + 2^{m-1} - 2^n|^{2H} + 2|2^m k - 2^n l + 2^{m-1}|^{2H} \\ &\quad +2|2^m k - 2^n l - 2^{n-1}|^{2H} - 4|2^m k - 2^n l + 2^{m-1} - 2^{n-1}|^{2H} \\ &\quad -|2^m k - 2^n l + 2^m - 2^n|^{2H} - |2^m k - 2^n l|^{2H} \\ &\quad -|2^m k - 2^n l + 2^m|^{2H} - |2^m k - 2^n l - 2^n|^{2H}). \end{aligned} \tag{3.13}$$

(b) For given m and n the correlation $r_d[m,n;k,l]$ of $d_m[k]$ decays as $O(|2^m k - 2^n l|^{2(H-2)})$ for all k and l such that $|2^m k - 2^n l| \neq 0$.

Proof: By repeated use of (2.1) with the Haar basis and given that $a_0[k] = X[k]$, one can express $a_m[k]$ as

$$a_m[k] = 2^{-\frac{m}{2}} \sum_{p=0}^{2^m-1} X[2^m k + p].$$

Then, with (1.6), the correlation can be determined as

$$\begin{aligned} r_a[m,n;k,l] &= E[a_m[k]a_n[l]] = 2^{-\frac{m+n}{2}} \sum_{p=0}^{2^m-1}\sum_{q=0}^{2^n-1} r[2^m k - 2^n l + p - q] \\ &= 2^{-\frac{m+n}{2}}\frac{\sigma^2}{2}\sum_{p=0}^{2^m-1}(|2^m k - 2^n l + p + 1|^{2H} - |2^m k - 2^n l + p|^{2H} \\ &\quad +|2^m k - 2^n l + p - 2^n|^{2H} - |2^m k - 2^n l + p - 2^n + 1|^{2H}) \\ &= 2^{-\frac{m+n}{2}}\frac{\sigma^2}{2}(|2^m k - 2^n l + 2^m|^{2H} - |2^m k - 2^n l|^{2H} \\ &\quad +|2^m k - 2^n l - 2^n|^{2H} - |2^m k - 2^n l + 2^m - 2^n|^{2H}). \end{aligned} \tag{3.14}$$

Since $d_m[k]$ and $a_{m-1}[k]$ are related by (3.9), the correlation of $d_m[k]$ can be expressed as

$$\begin{aligned} r_d[m,n;k,l] &= \frac{1}{2}[r_a(m-1,n-1;2k+1,2l+1)+r_a(m-1,n-1;2k,2l) \\ &\quad -r_a(m-1,n-1,2k+1,2l)-r_a(m-1,n-1,2k,2l+1)]. \quad (3.15) \end{aligned}$$

By substituting (3.14) into (3.15), the expression (3.13) follows and Part (a) is proved.

By letting $t = 2^m k - 2^n l$ and factoring t out of (3.13), the correlation of $d_m[k]$ is

$$\begin{aligned} r_d[m,n;k,l] &= \frac{\sigma^2}{2}2^{-\frac{m+n}{2}}|t|^{2H}(2|1+\frac{2^m-2^{n-1}}{t}|^{2H}+2|1+\frac{2^{m-1}-2^n}{t}|^{2H} \\ &\quad +2|1+\frac{2^{m-1}}{t}|^{2H}+2|1-\frac{2^{n-1}}{t}|^{2H}-4|1+\frac{2^{m-1}-2^{n-1}}{t}|^{2H} \\ &\quad -|1+\frac{2^m-2^n}{t}|^{2H}-1-|1+\frac{2^m}{t}|^{2H}-|1-\frac{2^n}{t}|^{2H}). \quad (3.16) \end{aligned}$$

By applying the Taylor series expansion (3.1) to (3.16), it is straightforward to show that

$$r_d(m,n;k,l) = \frac{\sigma^2}{2}2^{-\frac{m+n}{2}}|t|^{2H}\sum_{r=0}^{\infty}V(r)P(r)\frac{|t|^{-r}}{r!},$$

where

$$\begin{aligned} P(r) &= 2(2^m-2^{n-1})^r+2(2^{m-1}-2^n)^r+2(2^{m-1})^r+2(-2^{n-1})^r-4(2^{m-1}-2^{n-1})^r \\ &\quad -(2^m-2^n)^r-(2^m)^r-(-2^n)^r-\delta(r). \end{aligned}$$

Since

$$P(r) = 0 \quad \text{for} \quad r = 0,1,2,3,$$

the correlation of $d_m[k]$ decays as stated in Part (b). □.

Theorem 2 proves that the detail DWT coefficients are weakly correlated over both time and scale. The whitening effect is much stronger for the special case of normal Brownian motion ($H = 1/2$). By setting $H = 1/2$ in (3.13), then the correlation is zero as long as $2^m k - 2^n l \geq 2^n$ or $2^m k - 2^n l \leq -2^m$. Thus we have the following corollary.

Corollary 1 *Given $B[k]$ with $H = 1/2$, the detail wavelet coefficients $d_m[k]$ from the Haar transform are independent, i.e.*

$$r_d[m,n;k,l] = 0,$$

provided that m and n are fixed and that k and l are outside the region defined as

$$2^{n-m}l - 1 < k < 2^{n-m}(l+1).$$

This result is similar to one found in [3] for the case of the CWT and continuous fBm.

The whitening effect for general DFGN will be verified experimentally in Section 3.3. One advantage of using the DFGN and the Haar basis is that because the DWT coefficients are virtually uncorrelated for $0 < H < 1$ via Haar transform, the periodic extension of data problem is avoided. By comparing Part (b) of Theorem 2 to (2.4), we may say that the application of the discrete Haar transform to the DFGN, in a sense, behaves like the application of the continuous wavelet transform with the Daubechies D4 basis to the corresponding continuous-time fBm.

3.2 Extension to Higher Order Daubechies Filters

It seems that some results presented in Section 3.1 can be extended to wavelet bases of higher order. It is our conjecture that when the DFGN is passed through the DWT using a Daubechies filter [1] of length $2R$, the R vanishing moments of the filter should cancel out the first R terms in the correlation expansion of (3.2) so that the detail wavelet coefficients decay at a rate of

$$E[d_m[k]d_n[l]] = O(|2^m k - 2^n l|^{2(H-1-R)}). \tag{3.17}$$

In fact, a technique originated in [11] was used by Tewfik and Kim in [15] to verify the decay of (3.17). Their work is based on multiscale signal processing of sampled data, and it covers the special case of orthonormal wavelet basis. When the correlation structure of (1.6) is treated as a continuous function, the function will be continuously differentiable for $k > 1$. Based on [15], it can be argued that if a length $2R$ Daubechies filter is used for DWT implementation, the detail wavelet coefficients are bounded by

$$E[d_m[k]d_n[l]] \leq \sup_{0 \leq k', l' < 2R} \left| \frac{d^{2R} r[t]}{dt^{2R}} \right|_{t = 2^m k - 2^n l - k' + l'}. \tag{3.18}$$

By taking the $2R$ derivatives of (3.2), the asymptotic decay (3.17) is verified and experimental verification is provided in Section 3.3. Thus the DWT should be able to whiten the DFGN for any choice of wavelet basis with $R > 0$ vanishing moments.

It is believed, however, that only the Haar basis ($R = 1$) takes advantage of the self-similarity (1.5) of the fBm so that the variance progression is not biased. In the proof of Theorem 1, the variance progression (3.3) is a direct result of the fact that as the approximation coefficients become coarser, the correlation structure remains the same with the exception of a scaling factor. This nice feature does not occur for higher order filters. The bias in the variance progression is verified experimentally in Section 5.3. Even if the higher

order filters did not suffer from variance bias, they would be of limited value because of the windowing problem that results from the DWT implementation. Longer filters might create coefficients with correlation that decays faster than the Haar filters, but it is shown in Section 3.3 that the faster decay is not significant for real data.

3.3 Experimental Verification

To demonstrate the above discussion, the correlation of DFGN for fBm with $H = 0.8$ is examined. Figure 1 shows the theoretical autocovariance function of the DFGN process for lags -128 to 128 as given by (1.6). We clearly see that there is a rapid drop from lag 0 to other nonzero lags, but the function is slowly converging to zero. When a fBm realization of length 128 is treated as a vector and is put through a Haar transform, the output can also be treated as a vector where element 1 represents the coarsest approximation coefficient and elements 2 through 128 represent the detail coefficients from coarsest to finest. Because the approximation coefficient is of no interest, it is discarded and the resulting output vector is of length 127. By using (3.13), a theoretical covariance matrix is computed and displayed in Figure 2. Cross-correlation between overlapping time segments of different scales and the hyperbolic decay of the peaks are both evident in the figure. Finally, 256 realizations of fBm of length 128 were generated using the generative algorithm described in Section 5.1. These samples were put through the Haar transform and an average covariance matrix was computed. Figure 3 shows the matrix, and the figure displays a large diagonal peak with small off-diagonal elements. The variance progression is also evident. These experimental results validate the theory in Section 3.1.

To verify that higher order Daubechies filters do whiten the DFGN, we use the D4 and D16 bases to perform the same numerical experiment. In these experiments when the length of the filter became too long for the DWT implementation, a smaller filter is chosen just as in [16]. Figures 4 and 5 show the covariance matrices for the wavelet coefficients using the D4 and D16 bases, respectively. The whitening effect is verified. The faster decay of the peaks for the D16 filter, however, is not evident. The fact that a decay should occur seems more crucial than the actual rate of decay for real data. Besides, the higher order bases suffer from variance bias as will be tested in Section 5.3.

4 The Modified Algorithm

The theoretical results suggest that the Wornell and Oppenheim's algorithm can be improved by first computing the increments so that the problems of variance bias and periodic data extensions can be avoided. Then, we apply the Haar transform to the DFGN, compute the the average variance of detail coefficients $d_m[k]$ for each scale and use the EM algorithm to find a maximum likelihood estimate of H. It is important to note that the EM algorithm must be altered to reflect the variance progression of the noisy data.

To create a fractal estimator for noisy measurements, one must understand what happens to white noise when its increments are passed through the DWT. Let us assume that the additive white Gaussian noise $w[k]$ is independent of the $1/f$ process and has variance σ_w^2. Then, the white noise increment $w_i[k] = w[k+1] - w[k]$ has a autocorrelation structure of:

$$r_{w_i}[k] = \begin{cases} 2\sigma_w^2 & \text{if } k = 0 \\ -\sigma_w^2 & \text{if } |k| = 1 \\ 0 & \text{otherwise} \end{cases} .$$

One can verify that the process $w_i[k]$ is in fact a zero mean stationary Gaussian process characterized by the autocorrelation (1.6) with $H = 0$ and $\sigma^2 = 2\sigma_w^2$. It is important to note that even though the increment is of the form (1.6), white noise is not the same as fBm of $H = 0$ because the way DFGN is added up to generate fBm, the first element of the discrete-time fBm with $H = 0$ is correlated with all future samples. Since the increments, however, are equivalent, the same theory for the DFGN hold for $w_i[k]$. The variance progression of $w_i[k]$ can be determined from (3.3) by setting $H = 0$. Since the DWT is linear and white noise is independent of the fBm process, the wavelet coefficients from the white noise increment is independent of the wavelet coefficients of the DFGN, and the variance progression of noisy DFGN is

$$\sigma_m^2 = \text{var}[d_m[k]] = 2^{\gamma(m-1)}\sigma^2(2 - 2^\gamma) + 2^{-(m-1)}3\sigma_w^2, \tag{4.1}$$

where γ is defined in (3.4). In a sense, the modified EM algorithm, formulated according to (4.1), will separate two fBm signals i.e., one with $H = 0$ and the other one with unknown H.

The derivation of formulas for the Estimate Maximize (EM) algorithm can be found in Appendix A of [18] with trivial changes, and thus, will not be repeated here. Although the EM equations themselves do not change much for the modified algorithm, they are included

in the Appendix A for completeness. The new EM algorithm can be tuned for the same three modes as the original EM algorithm that was discussed in Section 2.

The Cramér-Rao bounds for the estimate of H can be computed through the Fisher information matrix, J. The J matrix changes depending on the mode of the algorithm, and are included in [18] for Wornell and Oppenheim's algorithm. For the modified algorithm, the matrices are no different than those in [18] except that a factor of 2^{-m} enters in the elements dealing with the estimation of σ_w^2. We discuss the derivation of the Cramér-Rao bounds for estimates of H and other related parameters in Appendix B.

The modified algorithm can be directly compared to a very common fractal estimation technique known as the variance estimator that was used as a control algorithm in [7]. It is basically a space domain version of the algorithm presented in [12]. The variance estimator uses the self-similar property (1.5). The variance of the increments are computed for different lags, i, and then regression analysis on a log-log scale is used to determine H. By looking at the proof of Theorem 1, one can see that in effect, the variance estimator performs the regression analysis on the approximation coefficients. In other words, the modified algorithm adds the wavelet filtering step of (2.2) to whiten the coefficients so that a maximum likelihood estimate of H is easy to formulate. Even without the maximum likelihood formulation, a regression analysis after the wavelet filtering step should provide for more accurate estimates because the coefficients are virtually independent.

5 Simulations

5.1 Generation of FBM

Many methods exist to generate approximations of sampled fBm such as the random midpoint displacement method [13] and the wavelet synthesis method of Wornell [17]. The midpoint displacement method fails to provide stationary increments for $H \neq 1/2$, and the wavelet method creates a nearly $1/f$ curve realization. The results of Section 4 suggest that another approach to wavelet synthesis is possible for which the DFGN is created first by the inverse DWT on independent samples and then summed up to create fBm curves. Another technique used in [7], however, does create a consistent fBm curve. This method creates the increments by using a Cholesky decomposition on the covariance matrix that can be found from (1.6). The Levinson recursion algorithm offers a very efficient way to perform the Cholesky decomposition [5]. The increments are then added up to form the fBm process. This decomposition method is used in our simulations because it provides

accurate fBm realizations. The accuracy does come at a price, however, because all other methods mentioned have a complexity of $O(N)$ while the Cholesky decomposition method's complexity is $O(N^2)$ due to the Levinson recursion.

5.2 Determination of SNR

The signal power of a fBm process has no clear meaning because the process is nonstationary. For the simulation work in [7], the signal strength was defined as the average squared value of the noise free test samples. Then, the SNR is just calculated by dividing the signal power by the noise variance. It is our experience that this definition does not accurately represent signal deterioration consistently for all values of H. It is known that curves of lower values of H will have smaller values than curves of larger values of H. In other words, for equal SNR, the noise strength would be larger for larger values of H. It is our belief that the increments hold the secret to fractal estimation and that it is the level of deterioration of the increments by noise which determines the ability of an estimator to provide accurate results. Following this motivation, we define the SNR as

$$\text{SNR} = 10 \log_{10} \frac{\sigma^2}{\sigma_w^2}. \tag{5.1}$$

Therefore, two sample fBm processes of the same length whose finest increments have the same variance will be corrupted by the same noise power for equal SNR no matter the value of H for the two processes.

The SNR as defined in (5.1) quantifies the quality of the noisy fBm measurements. For the modified algorithm, however, the effective SNR changes after the increments are calculated. From (4.1), it can be seen that the effective SNR is

$$\text{SNR} = 10 \log_{10} \frac{(2 - 2^{2H-1})\sigma^2}{3\sigma_w^2}$$

As a result, the degradation of the SNR which is defined as the loss of SNR is

$$\mathcal{D} = 10 \log_{10} \frac{2 - 2^{2H-1}}{3}. \tag{5.2}$$

The degradation is plotted versus H in Figure 6. One can see that the loss in SNR is only of much significance for $H \geq 0.9$, and even for $H = 0.9$, Section 5.3 shows that the modified algorithm provides more accurate results than that of Wornell and Oppenheim's algorithm. For processes found in nature, H will be less than 0.9 for most cases, and therefore, the degradation effect should not cause too many problems for the modified algorithm.

True	WO		Modified	
H	mean	std	mean	std
0.90	0.846	0.021	0.899	0.017
0.75	0.683	0.026	0.748	0.017
0.50	0.398	0.021	0.499	0.016
0.25	0.082	0.022	0.252	0.016

Table 1: Means and standard deviations for the H estimate with noise-free measurements in the noise-free mode

True	WO		Modified	
H	mean	std	mean	std
0.90	0.894	0.032	0.917	0.019
0.75	0.760	0.040	0.770	0.029
0.50	0.510	0.043	0.520	0.021
0.25	0.272	0.050	0.290	0.038

Table 2: Means and standard deviations for the H estimate with noise-free measurements in the noise search mode

5.3 Experimental Results

Wornell and Oppenheim's (WO) algorithm and our modified algorithm were compared using simulated fBm data. To implement the WO algorithm, the 16-tap Daubechies wavelet basis [1] was chosen, and any wavelet coefficients that could not be computed accurately were discarded. For our simulations, 64 samples of noise-free fBm of various lengths where $H = 0.25$, $H = 0.5$, $H = 0.75$, and $H = 0.9$ were created.

The WO and modified algorithms were first tested on the noise-free fBm data. The resulting mean and standard deviation of the value of H as estimated by the two algorithms under the noise-free assumption are given in Table 1. The problem of variance bias is very much evident in the WO algorithm. The standard deviation of the WO algorithm is also slightly larger. Table 2 shows the resulting statistics of the estimated parameter H when the two algorithms are tuned to search for a noise level. It appears that the WO algorithm, when searching for a noise floor, treats the variance bias as noise so that a less biased estimate of H can be found, but the standard deviation becomes significantly larger than that of the modified algorithm.

Next, white noise was added to the fBm data so that the SNR is $10dB$. The two algorithms were tested in the noise search mode. The RMS errors of the H estimate are plotted versus data length in Figures 7 through 10 for various values of H. It is clear

that the modified algorithm is superior for moderate data lengths while the two algorithms perform almost equally well at length 2048 .

Flandrin [3] showed that the bias in the variance progression, that leads to an underestimate of H, decreases as the scale becomes coarser. The EM algorithm, however, gives more credence to the variance estimates of finer scales because they contain more samples of data. As a result, the WO algorithm operating in the noise-free mode has difficulty in decreasing the error in the estimate of H as the number of samples increase. A simple fix to this problem is to just throw away the data form the finer scales before the EM algorithm is used. Figure 11 shows the mean value of the H estimate when the WO algorithm is implemented via the D4, D8, and D16 basis on noise free samples of fBm data with $H = 0.25$ and where the finest k scale detail coefficients are discarded. We see that excluding the finest scales do improve the estimate of H, even though the WO algorithm still underestimates H. Note also that the performance of the WO algorithm is not really sensitive to the choice of basis.

Since the method of finer scale exclusion offers a way to see if variance bias does exist in an algorithm, we also use this method to test the variance progression of the modified algorithm extended to higher order Daubechies filters. Figure 12 shows the result of finer scale exclusion using the same data as in the previous paragraph for the modified algorithm (the Haar basis) and it extension using the D4, D8, and D16 filter. The variance progression bias of higher order filters is evident in the figure.

We want to comment that throwing away the finer scales is not a practical fix to the bias problem, because the finer scales contain most of the data. For example, if data in the 3 finest scales are discarded, only 12.5% of the original data is used for the EM algorithm. As seen in Figure 11, the quality of the estimator is affected by the absence of the 3 finest scales for the D4 basis. A better way to handle the bias problem is to use an algorithm that does not suffer from the variance bias. The modified algorithm, in mode three, is such an algorithm, and its lack of variance bias is clearly seen in Figure 11.

6 Conclusions and Extensions

A theory about the DWT coefficients of the increments of the fBm using the Haar basis has been presented. It has also been shown that Wornell and Oppenheim's fractal estimation algorithm can be modified as a result of our new theory. The modified algorithm improves the accuracy of the H estimate for moderate data lengths of the fBm. For longer lengths,

both our algorithm and Wornell and Oppenheim's algorithm can find very good estimates. For short data lengths of the fBm in additive noise, the modified algorithm is still unreliable, and it is so far not clear how to improve the fractal estimator for short data lengths. Although highly regular filters may zero out terms in the Taylor series expansion of the autocorrelation of DFGN, they cause a bias in variance progression. How to avoid the bias of high-order filters is also of interest.

Appendix A: The Estimate Maximize (EM) Algorithm

Note that some simple changes to the original equations occur because the definition for scale m is reversed. Other changes result from the needed modifications. To make the notation easier, the following terms are defined:

$$\beta = 2^{\gamma}, \tag{A.1}$$

$$\sigma'^2 = (2 \cdot 2^{-\gamma} - 1)\sigma^2, \tag{A.2}$$

$$\sigma'^2_w = 6\sigma^2_w, \tag{A.3}$$

so that the variance progression has the simple form of

$$\sigma^2_m = \sigma'^2 2^{\gamma m} + \sigma'^2_w 2^{-m},$$

where $\gamma = 2H - 1$. The EM algorithm will be presented for the usual case where $2^M + 1$ noisy fBm samples are available. For a more general scenario, only the equation describing $N(m)$ needs to be altered. To begin, given $2^M + 1$ samples of fBm data, 2^M samples of DFGN are computed and then passed through the DWT to provide the detail wavelet coefficients. These coefficients control the likelihood function for which the EM algorithm searches a minimum. The likelihood function is

$$L(\Theta) = -\frac{1}{2}\sum_{m=1}^{M} N(m)\frac{\hat{\sigma}^2_m}{\sigma^2_m} + \ln(2\pi\sigma^2_m),$$

where

$$\hat{\sigma}^2_m = \frac{1}{N(m)}\sum_{k=0}^{N(m)-1} d_m[k]^2,$$

$$N(m) = 2^{M-m},$$

$$\Theta = \{\beta, \sigma'^2, \sigma'^2_w\},$$

and where σ^2_m is given by (4.1) with $1 \leq m \leq M$. The iterative equations for step l used to find the minimum are divided in an estimate (E) step and a maximize (M) step. For the E step, the algorithm estimates the noise and signal portions of the wavelet coefficients separately by the following equations:

$$S^w_m(\hat{\Theta}^{(l)}) = A_m(\hat{\Theta}^{(l)}) + B^w_m(\hat{\Theta}^{(l)})\hat{\sigma}^2_m, \tag{A.4}$$

$$S^x_m(\hat{\Theta}^{(l)}) = A_m(\hat{\Theta}^{(l)}) + B^x_m(\hat{\Theta}^{(l)})\hat{\sigma}^2_m, \tag{A.5}$$

where

$$A_m(\hat{\Theta}^{(l)}) = \frac{\hat{\sigma'}_w^{2(l)}[2]^{-m}\hat{\sigma'}^{2(l)}[\hat{\beta}^{(l)}]^m}{\hat{\sigma'}_w^{2(l)}[2]^{-m} + \hat{\sigma'}^{2(l)}[\hat{\beta}^{(l)}]^m}, \tag{A.6}$$

$$B_m^w(\hat{\Theta}^{(l)}) = \left(\frac{\hat{\sigma'}_w^{2(l)}[2]^{-m}}{\hat{\sigma'}_w^{2(l)}[2]^{-m} + \hat{\sigma'}^{2(l)}[\hat{\beta}^{(l)}]^m}\right)^2, \tag{A.7}$$

$$B_m^x(\hat{\Theta}^{(l)}) = \left(\frac{\hat{\sigma'}^{2(l)}[\hat{\beta}^{(l)}]^m}{\hat{\sigma'}_w^{2(l)}[2]^{-m} + \hat{\sigma'}^{2(l)}[\hat{\beta}^{(l)}]^m}\right)^2. \tag{A.8}$$

The M step updates the estimates by

$$\hat{\beta}^{(l+1)} \leftarrow \sum_{m=1}^{M} C_m N(m) S_m^x(\hat{\Theta}^{(l)})\beta^{M-m} = 0, \tag{A.9}$$

$$\hat{\sigma'}^{2(l+1)} = \frac{\sum_{m=1}^{M} N(m) S_m^x(\hat{\Theta}^{(l)})[\hat{\beta}^{(l+1)}]^{-m}}{\sum_{m=1}^{M} N(m)}, \tag{A.10}$$

$$\hat{\sigma'}_w^{2(l+1)} = \frac{\sum_{m=1}^{M} N(m) S_m^w(\hat{\Theta}^{(l)})[2]^m}{\sum_{m=1}^{M} N(m)}, \tag{A.11}$$

where

$$C_m \doteq \frac{m}{\sum_{m=1}^{M} mN(m)} - \frac{1}{\sum_{m=1}^{M} N(m)}. \tag{A.12}$$

Once $\hat{\beta}^{(l)}$ converges to $\hat{\beta}_{ML}$ and the other two parameters converge to their maximum likelihood solutions, the estimates of parameters H, σ^2, and σ_w^2 are determined by the inverse of (A.1) through (A.3), i.e.

$$\hat{H}_{ML} = \frac{1}{2}(\log_2(\hat{\beta}_{ML}) + 1),$$

$$\hat{\sigma}^2_{ML} = \frac{\hat{\sigma'}^2_{ML}}{2\hat{\beta}_{ML}^{-1} - 1},$$

$$\hat{\sigma}^2_{wML} = \frac{1}{6}\hat{\sigma'}^2_{wML}.$$

Note that the new EM algorithm is basically the same as the one given in [18] except that $2^m\sigma_w^2$ is substituted for σ_w^2 and the definition of β is changed slightly. Also note that in this work, only the estimate of H is of importance.

The new EM algorithm, just as the old one, can be tuned for three modes. The equations given above are for the case that the noise level is unknown. If $\sigma_w^2 > 0$ is known, then $\hat{\sigma'}_w^{2(l)} = \sigma'^2_w$ and (A.4), (A.7), and (A.11) are not needed. Finally, for the case that it is known that $\sigma_w^2 = 0$, then only (A.9) and (A.10) are needed (where $S_m^x(\hat{\Theta}^{(l)}) = 1$) and no iterations are necessary.

Appendix B: The Cramér-Rao Bound

The Fisher information matrix matrix J is defined to bound the estimation error of γ. For the case that the noise level is unknown, we can derive

$$\mathbf{J} = \sum_{m=1}^{M} \frac{N(m)}{2(\sigma_m^2)^2} \begin{pmatrix} [\ln(2^{-m})\sigma'^2\beta^m]^2 & -\ln(2^{-m})\sigma'^2[\beta^m]^2 & -2^{-m}\ln(2^{-m})\sigma'^2\beta^m \\ -\ln(2^{-m})\sigma'^2[\beta^m]^2 & [\beta^m]^2 & 2^{-m}\beta^m \\ -2^{-m}\ln(2^{-m})\sigma'^2\beta^m & 2^{-m}\beta^m & [2^{-m}]^2 \end{pmatrix}. \tag{B.1}$$

The bounds on the estimation error for unbiased estimates are

$$\mathrm{var}\hat{\gamma} \geq J^{11}, \quad \mathrm{var}\hat{\sigma'}^2 \geq J^{22}, \quad \mathrm{var}\hat{\sigma'}_w^2 \geq J^{33},$$

where J^{ii} represent element (i,i) in $\mathbf{J}^{-1}$. Since the estimation of H is important for this work, the bound on the estimate $H = \frac{1}{2}(1+\gamma)$ is

$$\mathrm{var}\hat{H} \geq \frac{1}{4}J^{11}.$$

Note that the above bounds may not be of great help because they depend on the parameter being estimated. In particular, there are no close form solutions for the inverse of J in (B.1), and as a result, the Cramér-Rao bounds must be calculated separately for each new scenario.

For the case that $\sigma_w^2 > 0$ is known, the Fisher information matrix is just the 2×2 principle submatrix of J in (B.1). The estimation error bound can be computed accordingly. For this information matrix the noise term is discarded, and as a result, the matrix has the same form as the one that results from the Wornell and Oppenheim algorithm. Again for this case, the bounds depend on the parameters being estimation and need to be computed for every new situation.

The Fisher information matrix for the case that the noise is known to be nonexistent is easily computed from the matrix resulting from case 2 in the previous paragraph. The J matrix is exactly the same as the one that appears for the Wornell and Oppenheim algorithm with the exception of a sign change on the off diagonal terms, i.e.

$$\mathbf{J} = \begin{pmatrix} \frac{(\ln 2)^2}{2}\sum_{m=1}^{M} m^2 N(m) & \frac{\ln 2}{2\sigma'^2}\sum_{m=1}^{M} mN(m) \\ \frac{\ln 2}{2\sigma'^2}\sum_{m=1}^{M} mN(m) & \frac{1}{2\sigma'^4}\sum_{m=1}^{M} N(m) \end{pmatrix}. \tag{B.2}$$

This information is useful because it does not depend on the parameter β, the bound for the modified algorithm is exactly the same as that of the original algorithm. The new algorithm, however, is more likely to reach the bound because there is much less bias in the estimates. This fact is also true for the two other cases mentioned earlier.

References

[1] I. Daubechies, "Orthonormal bases of compactly supported wavelets," *Communications on Pure and Applied Mathematics*, Vol. 41, pp. 909–996, Nov. 1988.

[2] P. Flandrin, "On the spectrum of fractional Brownian motions," *IEEE Trans. on Information Theory*, Vol. 35, pp. 197–199, Jan. 1989.

[3] P. Flandrin, "Wavelet analysis and synthesis of fractional Brownian motion," *IEEE Trans. on Information Theory*, Vol. 38, pp. 910–917, Mar. 1992.

[4] N. Gache, P. Flandrin, and D. Garreau, "Fractal dimension estimators for fractal Brownian motions," in *Proc. int. conf. Acoustic, Speech, Signal Processing*, pp. 3557–3560, Mar. 1991.

[5] S. Haykin, *Adaptive Filter Theory*, Englewood Cliffs, NJ: Prentice Hall, Inc., 1991.

[6] M. S. Keshner, "$1/f$ noise," *Proceedings of the IEEE*, Vol. 70, pp. 212–218, Mar. 1982.

[7] T. Lundahl, W. J. Ohley, S. M. Kay, and R. Siffert, "Fractional Brownian motion: A maximum likelihood estimator and its application to image texture," *IEEE Trans. on Medical Imaging*, Vol. 5, pp. 152–161, Sept. 1986.

[8] S. G. Mallat, "A theory for multiresolution signal decomposition: the wavelet representation," *IEEE Trans. on Pattern Analysis and Machine Intelligence*, Vol. 11, pp. 674–693, July 1989.

[9] B. Mandelbrot, *The Fractal Geometry of Nature*, San Francisco, CA: Freeman, 1982.

[10] B. Mandelbrot and J. W. V. Ness, "Fractional Brownian motions, fractional noises and applications," *SIAM Review*, Vol. 10, pp. 422–437, Oct. 1968.

[11] Y. Meyer, *Ondelettes et Operateurs*, Paris, France: Herman, 1990.

[12] A. P. Pentland, "Fractal-based description of natural scenes," *IEEE Trans. on Pattern Analysis and Machine Intelligence*, Vol. 6, pp. 661–674, Nov. 1984.

[13] H. O. Petigen and D. Saupe, eds., *The Science of Fractal Images*, New York: Springer-Verlag, 1988.

[14] A. H. Tewfik and M. Deriche, "Maximum likelihood estimation of the fractal dimensions of stochastic fractals and Cramér-Rao bounds," in *Proc. int. conf. Acoustic, Speech, Signal Processing*, pp. 3381–3384, Mar. 1991.

[15] A. H. Tewfik and M. Kim, "Fast multiscale statistical signal processing algorithms." To appear in *IEEE Trans. on Signal Processing.*

[16] A. H. Tewfik and M. Kim, "Correlation Structure of discrete wavelet coefficients of fractional Brownian motion," *IEEE Trans. on Information Theory*, Vol. 38, pp. 904–909, Mar. 1992.

[17] G. W. Wornell, "A Karhunen-Loève-like expansion for $1/f$ processes via wavelets," *IEEE Trans. on Information Theory*, Vol. 36, pp. 859–861, July 1990.

[18] G. W. Wornell and A. V. Oppenheim, "Estimation of fractal signals from noisy measurements using wavelets," *IEEE Trans. on Signal Processing*, Vol. 40, pp. 611–623, Mar. 1992.

Figure Captions

Figure 1: Autocorrelation of DFGN with $H = 0.8$.

Figure 2: Magnitude of entries of the theoretical covariance matrix of the wavelet coefficients with the Haar basis and $H = 0.8$.

Figure 3: Magnitude of entries of the experimental covariance matrix of the wavelet coefficients with the Haar basis and $H = 0.8$.

Figure 4: Magnitude of entries of the experimental covariance matrix of the wavelet coefficients with the Daubechies D4 basis and $H = 0.8$.

Figure 5: Magnitude of entries of the experimental covariance matrix of the wavelet coefficients with the Daubechies D16 basis and $H = 0.8$.

Figure 6: Degradation of SNR for the modified algorithm.

Figure 7: RMS error of the estimate for $H = 0.9$.

Figure 8: RMS error of the estimate for $H = 0.75$.

Figure 9: RMS error of the estimate for $H = 0.5$.

Figure 10: RMS error of the estimate for $H = 0.25$.

Figure 11: Mean value of H of various estimators with fine scale exclusion for $H = 0.25$.

Figure 12: Mean value of H of various DFGN estimators with fine scale exclusion for $H = 0.25$.

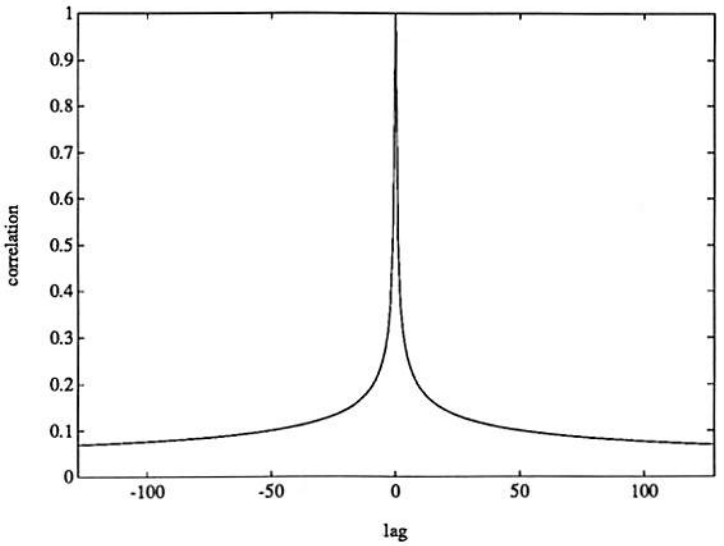

Figure 1: Autocorrelation of DFGN with $H = 0.8$.

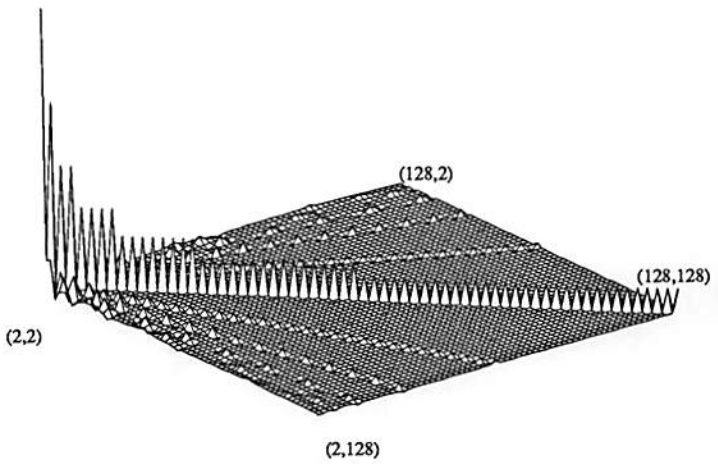

Figure 2: Magnitude of entries of the theoretical covariance matrix of the wavelet coefficients with the Haar basis and $H = 0.8$.

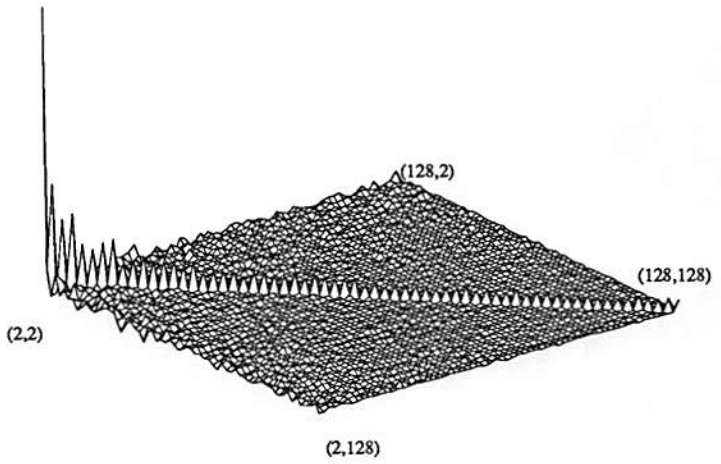

Figure 3: Magnitude of entries of the experimental covariance matrix of the wavelet coefficients with the Haar basis and $H = 0.8$.

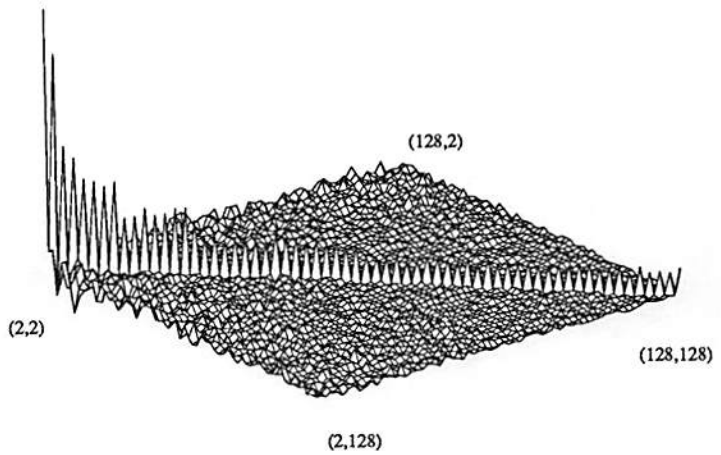

Figure 4: Magnitude of entries of the experimental covariance matrix of the wavelet coefficients with the Daubechies D4 basis and $H = 0.8$.

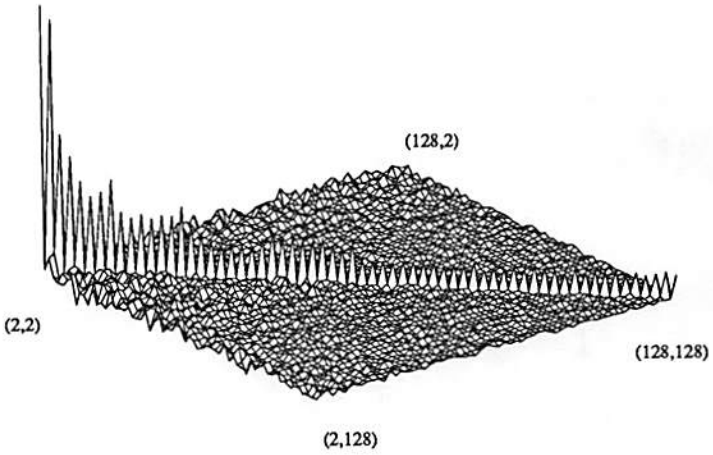

Figure 5: Magnitude of entries of the experimental covariance matrix of the wavelet coefficients with the Daubechies D16 basis and $H = 0.8$.

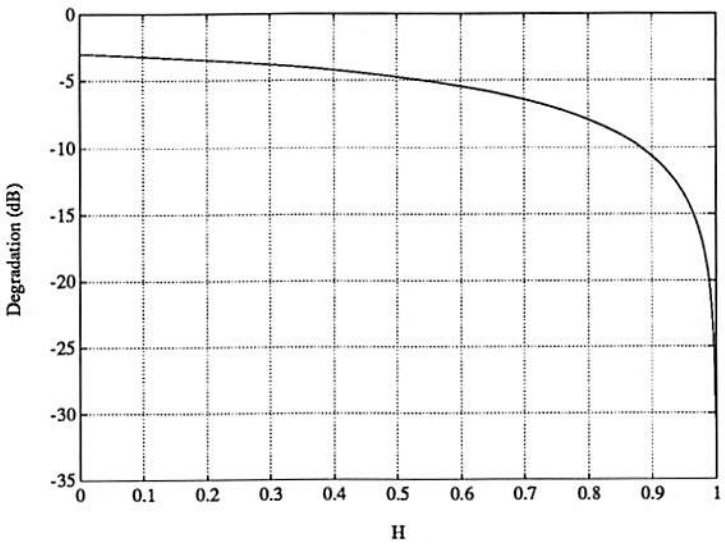

Figure 6: Degradation of SNR for the modified algorithm.

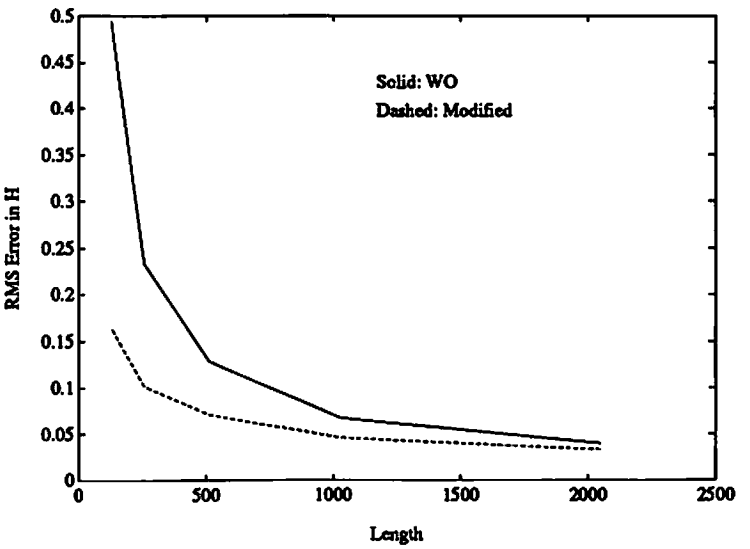

Figure 7: RMS error of the estimate for $H = 0.9$.

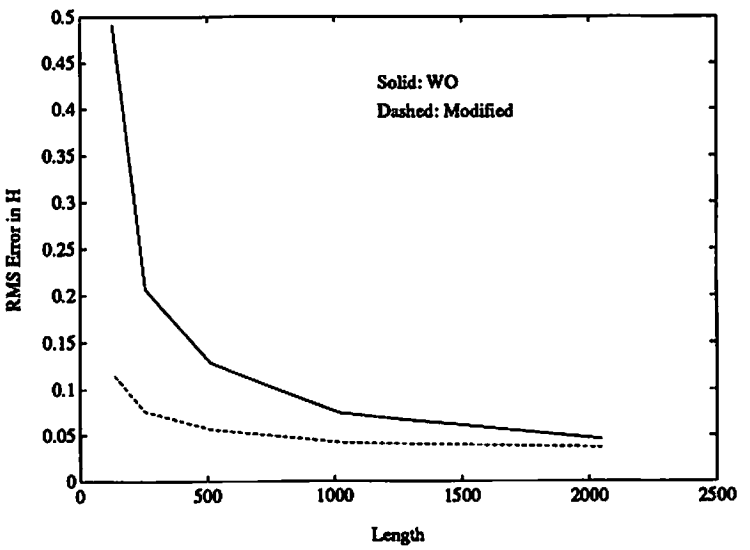

Figure 8: RMS error of the estimate for $H = 0.75$.

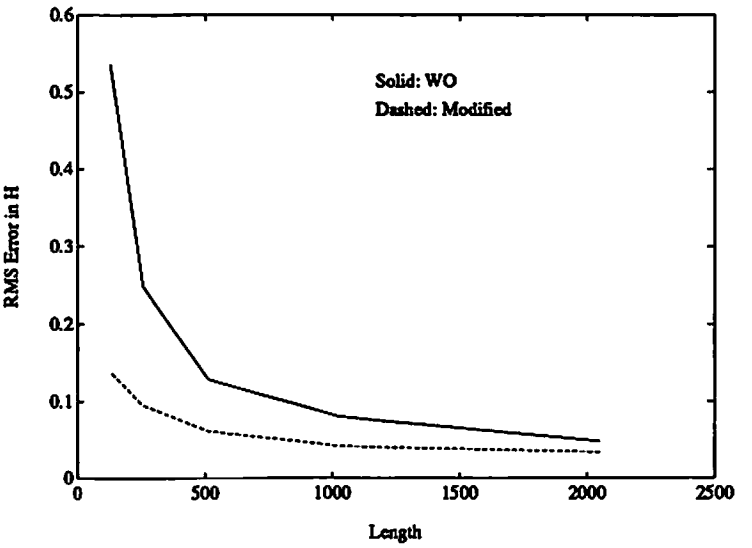

Figure 9: RMS error of the estimate for $H = 0.5$.

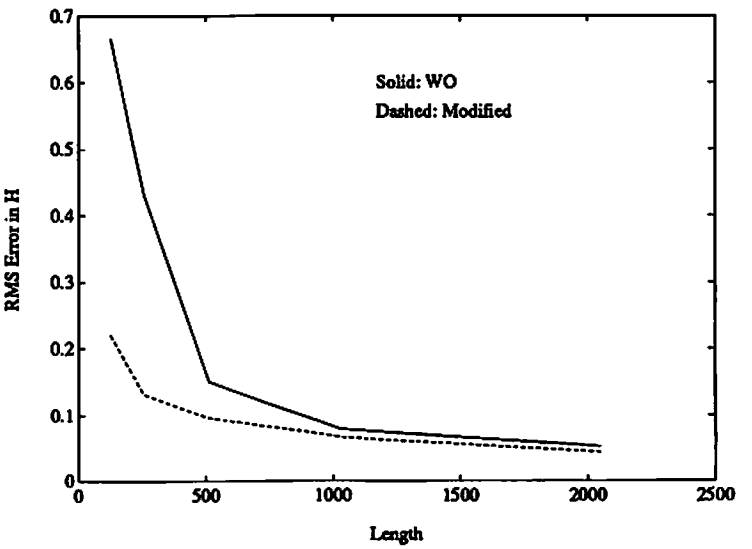

Figure 10: RMS error of the estimate for $H = 0.25$.

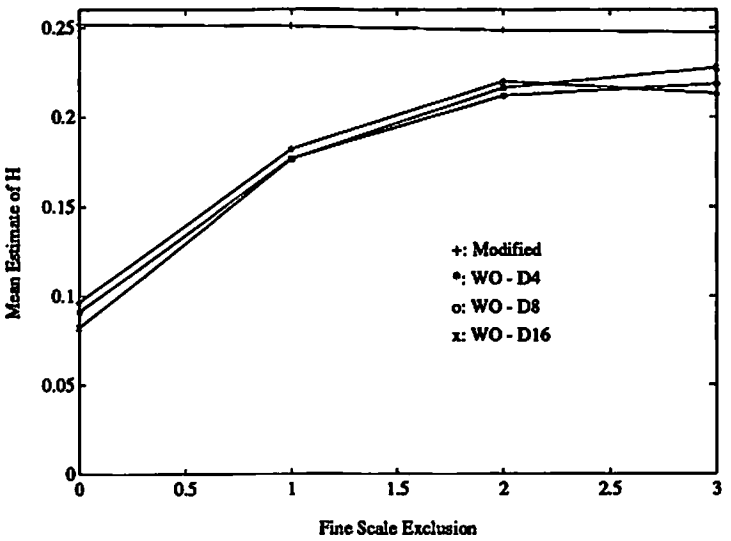

Figure 11: Mean value of H of various estimators with fine scale exclusion for $H = 0.25$.

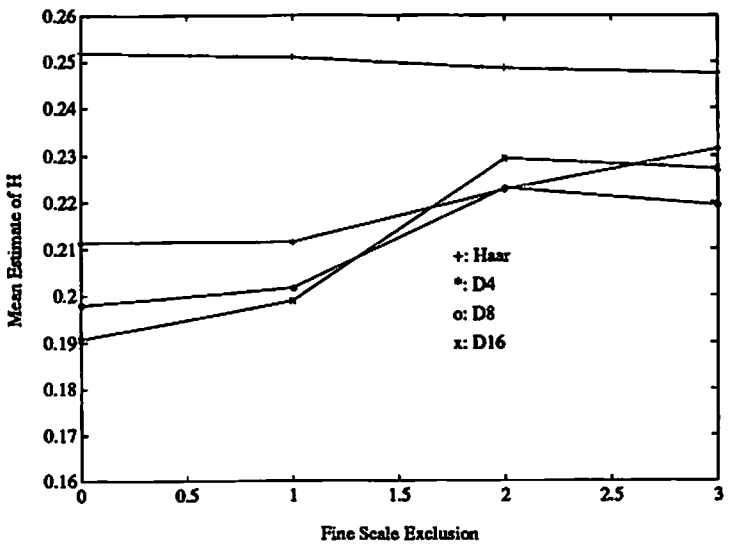

Figure 12: Mean value of H of various DFGN estimators with fine scale exclusion for $H = 0.25$.